Evidence for Site-Specific Reversible Hydrogen Adsorption on Graphene by Sum-Frequency Generation Spectroscopy and Density Functional Theory

Huda AlSalem,[1,2,3] Xavier Just-Baringo,[1] Igor Larrosa,[1] Umberto Monteverde,[4] Xingxing Jiang,[5] Yexin Feng,[5] Sven P. K. Koehler[6*]*

1 School of Chemistry, The University of Manchester, Oxford Road, Manchester, M13 9PL, United Kingdom.

2 Photon Science Institute, The University of Manchester, Oxford Road, Manchester, M13 9PL, United Kingdom.

3 School of Chemistry, Princess Nourah bint Abdulrahman University, Riyadh, Saudi Arabia.

4 School of Chemical Engineering and Analytical Sciences, The University of Manchester, Oxford Road, Manchester, M13 9PL, United Kingdom.

5 School of Physics and Electronics, Hunan University, Changsha 410082, P. R. China.

6 School of Science and the Environment, Manchester Metropolitan University, Chester Street, Manchester, M1 5GD, United Kingdom.

AUTHOR INFORMATION

Corresponding Authors

*Huda AlSalem (huda.alsalem@postgrad.manchester.ac.uk) *Sven P. K. Koehler (s.koehler@mmu.ac.uk)

ABSTRACT

We have characterized the C-H stretching vibrations of hydrogenated graphene on gold substrates using vibrational sum-frequency generation (SFG) spectroscopy. These C-H stretches are red-shifted as compared to aliphatic C-H stretches, and SFG signal intensities of the C-H vibrational features increase with increasing hydrogen coverage. By comparison with density-functional theory (DFT) calculations, we conclude that hydrogen atoms covalently attach to the graphene lattice from above the graphene sheet; preferential binding motifs are dimers in the *ortho* and *para* position. SFG spectroscopy is hence not only able to detect hydrogen atoms on graphene at sub-monolayer coverage, but it can also serve to obtain relative information about the surface coverage, and in combination with DFT can reveal information about binding motifs.

1. INTRODUCTION

Graphene's unusual physical, chemical, and mechanical properties have received appreciable attention over the past decade or two,[1] and it is predicted that graphene can find use in a range of applications.[2] Pristine graphene, however, is a semi-metal and does not possess a band gap, which limits its suitability for some applications in photonics and (opto-)electronics.[3,4] Zhang *et al.* called graphene's lack of a band gap its *Achilles' heel* "which seriously reduces [graphene's] ability to switch current on and off in transistors".[5] Thus, there has been a drive towards altering graphene's electronic properties in order to engineer a band gap, which can be done by e.g. modifying its chemical structure. For example, chemical functionalizations with nitrogen,[6,7] halogen,[8–10] oxygen,[11,12] as well as aryl diazonium salts[13–17] have been performed to tune the band gap of graphene.

Hydrogenation of graphene is the most commonly employed chemical method to tune the band gap of graphene,[3,18–23] and to facilitate proton transfer through graphene sheets.[24–26] Hydrogenation is also the simplest modification of graphene, and can be more straightforwardly modelled *in silico* compared to modifications with functional groups containing more and/or heavier atoms. There is also an application-driven interest in hydrogenated graphene as it can potentially act as a hydrogen storage medium as hydrogenated graphene can undergo dehydrogenation through annealing at modest temperatures.[27–29]

A number of experimental techniques have been employed in order to characterize covalently-functionalized graphene derivatives, but most of these have some drawbacks, especially when it comes to hydrogenated graphene. Raman spectroscopy, by far the most commonly employed technique for the characterization of graphene, only detects phonon vibrations of pristine (G and

2D peaks) or defect (D peak) graphene, but does not detect the C-H stretches directly.[30–32] X-ray photoelectron spectroscopy (XPS) cannot detect hydrogen atoms on graphene,[33] and any sp^3 carbon atoms detected may be a result of defect sites or due to carbon-containing impurities.[34] Scanning probe microscopies such as STM can provide detailed information,[13,21] but are limited to small sample areas, whereas linear spectroscopic techniques such as reflection absorption infra-red spectroscopy (RAIRS) can probe large areas, but are not surface selective, and close to their detection limit at sub-monolayer coverages, which functionalized graphene samples inherently are.

Non-linear spectroscopies such as sum-frequency generation (SFG) spectroscopy, however, have become a powerful tool to perform vibrational spectroscopy on interfaces with sub-monolayer coverage.[35–38] Its intrinsic surface specificity and sensitivity also make SFG a great choice to characterize vibrations on modified graphene surfaces. Su *et al.* and Holroyd *et al.* detected polymer residues on transferred graphene using SFG spectroscopy,[39,34] and AlSalem *et al.* detected aromatic C-H stretches of covalently functionalized phenyl-decorated graphene, and extracted absolute surface coverages with phenyl groups.[17]

Hydrogenated graphene itself has also been investigated by Kim *et al.* who have identified C-H stretches of hydrogenated graphene grown on Ir(111) single crystals at 2563 cm^{-1} and 2716 cm^{-1} using their picosecond SFG setup; these stretches were assigned to dimers in the *para* and *ortho* position, respectively.[19] Subsequent experiments by the same group using an elegant combination of hydrogenation and deuteration to avoid the annihilation of the SFG signal due to centro-symmetry revealed C-H vibrational frequencies between 2840 cm^{-1} and 2850 cm^{-1}.[40,41] Bisson and co-workers observed vibrational features of hydrogenated graphene at 2460 cm^{-1} and at 2702 cm^{-1} (at a resolution of 30 cm^{-1}) using high-resolution electron energy loss spectroscopy

(HREELS) and assigned the former peak to hydrogen dimers, while the 2702 cm^{-1} peak has been assigned to hydrogen clusters in a chair-like graph*ane* configuration.[42]

Further attention has been paid to the issue of hydrogenated graphene from a theoretical standpoint using density-function theory (DFT). Sakong and Kratzer calculated the vibrational modes and binding energies of hydrogen adsorbed on free-standing graphene;[43] they calculated the vibrational stretches to occur at 2692 cm^{-1}, 2883/2849 cm^{-1} and 2764/2746 cm^{-1} for isolated hydrogen, two hydrogen atoms on the same (*cis*) side in *ortho*, and in *para* position, respectively, with a shift for hydrogenation from opposite (*trans*) sides of a few tens of wavenumbers at most.

It is intuitive that hydrogenation with a single H atom per benzene ring is unlikely as this would (in the case of a radical attack) leave a free electron behind; this is backed by the small binding energies calculated for these configurations, and in fact for all systems with odd numbers of hydrogen atoms per benzene ring.[43,44] Instead, hydrogenation with a single H atom encourages the formation of a second C-H bond, which is unlikely to occur in the meta position,[43,45] but there is no agreement as to whether the second H atom attaches preferentially in the *ortho* or *para* position. While almost all prior measurements and calculations agree that C-H vibrational frequencies are red-shifted in hydrogenated graphene compared to aliphatic C-H stretches, there is no agreement on whether dimers or clusters of higher hydrogen count form, nor is there an agreement as to whether hydrogenation occurs from only one side of the graphene sheet, or from both sides. We specifically address these questions in this work through a combination of broadband-SFG spectroscopy and density functional theory; furthermore, we are able to directly correlate the intensities of our spectroscopic signatures with the hydrogen coverage on graphene.

2. METHODS

2.1. Sample Preparation. Graphene was grown in-house by chemical vapor deposition (CVD) on a Cu foil; the newly-formed monolayers were subsequently transferred onto a 50 nm thick layer of gold which had been evaporated onto a borosilicate glass substrate; the graphene transfer is facilitated using PMMA as a transfer agent. The Birch reduction was carried out following the method used by Sheehan *et al.*[46] Ammonia gas was liquified in a cold-finger condenser at -78°C under a nitrogen atmosphere. Solid lithium metal was added to the liquid, giving rise to the intense blue colour synonymous with electrons solvated in ammonia. We synthesised two sets of four graphene samples each, and quenched the solution by addition of 20 mL of ethanol (which provided the protons which covalently attach to graphene) at four different reactions times, namely 45 s, 120 s, 300 s, and 360 s, to achieve different hydrogenation coverages. The samples were washed with deionised water and acetone and dried under a gentle stream of nitrogen before being transferred in air to the laser setup.

2.2. Optical setup. The laser setup has been described in detail previously.[17] An 800 nm, ~120 fs duration laser pulse from a Ti:Sapphire amplifier (Coherent Legend Elite-F-HE) is split into two beams, one of which is used as the VIS beam in our SFG setup, while the other is steered into an OPerA Solo Optical Parametric Amplifier (Coherent). The latter beam produces an IR beam tuneable from 1100-20000 nm via non-collinear difference frequency generation with a ~120 fs pulse duration and a repetition rate of 1 kHz. The IR pulse envelope has a width of ~250 cm^{-1}, ensuring that we can acquire spectra over a fairly broad spectral range with a single shot. Both beams are *p*-polarised and steered onto the sample through a CaF_2 prism. The polarisation of the beams can be altered using

a combination of polarisation cubes and half-wave plates. The angles of incidence chosen were 63° and 51° from the surface normal, however, angles were chosen such that total internal reflection did not occur at the CaF_2 prism surface. All spectra were recorded with a time-asymmetric visible pulse delayed by 1 ps with respect to the IR beam for non-resonant background suppression,[47] typically observed in SFG experiments when using metal surfaces such as gold, and due to an upconversion process initiated by the IR pulse; this leads to a resolution of our spectrometer of ~15 cm^{-1}. In our case and owing to the weak signal, the non-resonant contribution cannot be suppressed completely, and hence interferes with the resonant peak itself. The time-asymmetric visible upconversion pulse was formed from the time-symmetric femtosecond pulses with the aid of an air-spaced Fabry-Perot etalon. The generated SF beam was subsequently steered into a spectrograph (Shamrock 750, Andor Technology) coupled to an intensified charge-coupled device (ICCD) camera (iStar ICCD DH 374, Andor Technology). Spectra were recorded at room temperature with typical acquisition times of around 2 min.

2.3. Computational Method. Density functional theory (DFT) was used to calculate vibrational frequencies of hydrogen atoms covalently bound to graphene. The Vienna *ab initio* simulation package (VASP) was employed,[48] and a plane-wave basis set with 3D periodic boundary conditions described electronic interactions. The projector augmented-wave (PAW) approximation described valence and core electronic interaction.[49] Exchange and correlation effects were added within the generalised-gradient approximation (GGA) via the Perdew-Burke-Erzenhof (PBE) functional.[50] The simulated system consisted of 6 × 6 unit cells of graphene on top of 4 layers of Au(111) with a vacuum region of about 12 Å. The total energies of the overall systems were minimised

using the conjugate gradient method with a force tolerance of 10^{-5} eV/Å.[51] The energies of all atoms were converged to within 10^{-6} eV. A Γ-centered 4 × 4 × 1 mesh of the Monkhorst−Pack *k* points and a cut-off energy of 500 eV were employed, which are sufficient to converge the total energy of the system. Hydrogen atoms were chemically adsorbed to C atoms of the graphene sheet, and the vibrational frequencies were subsequently calculated with optimized geometries. The anharmonic vibrational spectra were obtained by Fourier transform of the velocity autocorrelation function, which was calculated from *ab initio* molecular dynamics (MD) simulations at 300 K for 8 ps.

3. RESULTS AND DISCUSSION

A first indication that the Birch reduction indeed induced some chemistry on graphene comes from the Raman spectra shown in Figure 1. These spectra were recorded before and after hydrogenation, and after thermal annealing of the hydrogenated sample. The presence of the D peak around 1350 cm^{-1}, the decrease of the 2D peak around 2680 cm^{-1} and the presence of the D+D' peak around 2920 cm^{-1} indicate an increasing defect density within the graphene sheet. In addition, following the model proposed by Lucchese *et al*.[30] and applying the corrected parameters used by Strano *et al.,*[52] the ratio of the Raman intensities of the D peak to the G peak (I_D/I_G) can be used to estimate the defect densities of the graphene samples (see SI for more information). We calculate an average defect separation of 2.58 nm, 2.04 nm, 1.83 nm, and 1.66 nm for the 45 s, 120 s, 300, and 360 s reaction times, respectively; this corresponds to coverages of 1.5%, 2.4%, 3%, and 3.6% for the four samples *if* all defects were due to hydrogen adsorbing onto graphene; similar coverages were reported by Hu and coworkers.[21] It has to be stressed, however, that these coverages are strictly speaking only defect densities in the graphene lattice, and *not* hydrogen coverages, as Raman spectroscopy does not detect the C-H vibrations

directly. Figure 1 (e) also shows the Raman spectrum of a restored graphene sample after annealing the hydrogenated sample at 200°C under an inert N_2 atmosphere for 2 hours. This is

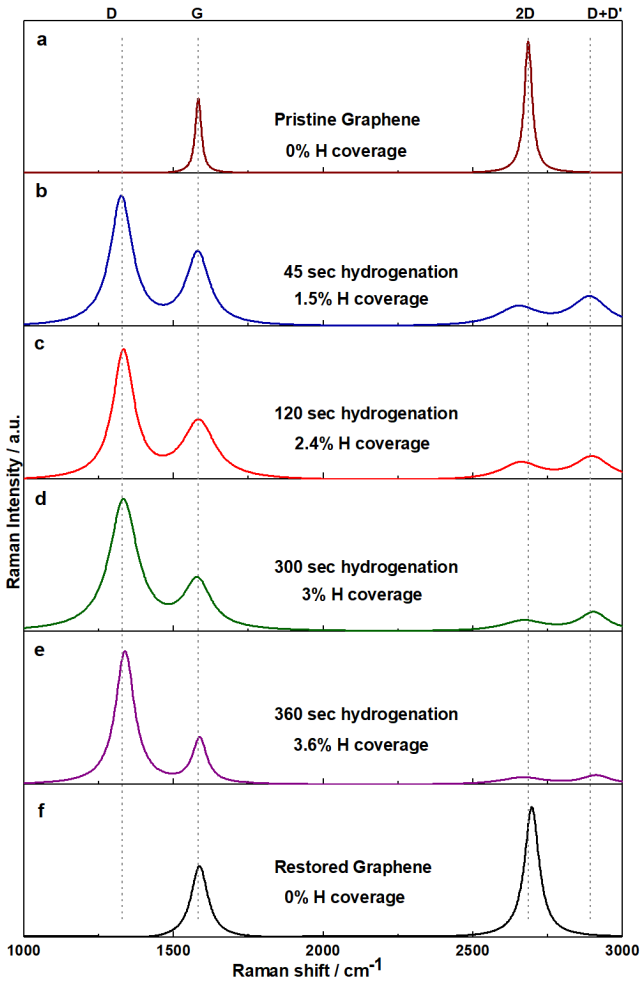

significant as the disappearance of the D peak demonstrates the complete reversibility of the hydrogenation process.

Figure 1. Raman spectra for a) pristine and b) - e) hydrogenated graphene. The increase of the D peak intensity in the hydrogenated samples indicates an increase in the defect density; f) the same hydrogenated graphene sample but restored to pristine graphene through annealing in an inert N_2 atmosphere.

While the Raman spectra in Figure 1 only indicate the presence of defects in the graphene lattice, the SFG spectrum in Figure 2 directly results from the C-H stretches of hydrogenated graphene. The raw spectrum (with the non-resonant background subtracted) in Figure 2 is noisy due to the low hydrogen surface coverage (upper limit of 1-4% according to the Raman intensities) and the low non-linear susceptibility of the C-H vibrations. The raw spectra were hence fitted taking into account the interaction between the resonant and non-resonant contributions to the overall SFG signal as described in equation 1 and shown in Figure 2,[36]

$$I = A_0 \, e^{i\Phi} + \left| \sum_{i=1}^{n} \frac{A_n}{\omega_n - \omega_{IR} - i\Gamma_n} \right|^2 \qquad \text{eqn. 1}$$

where $A_0 e^{i\Phi}$ is the non-resonant contribution, A_n the amplitude, ω_{IR} is the center frequency of the IR pulse, and ω_n and Γ_n are the frequency and linewidth of the n^{th} corresponding vibrational mode.

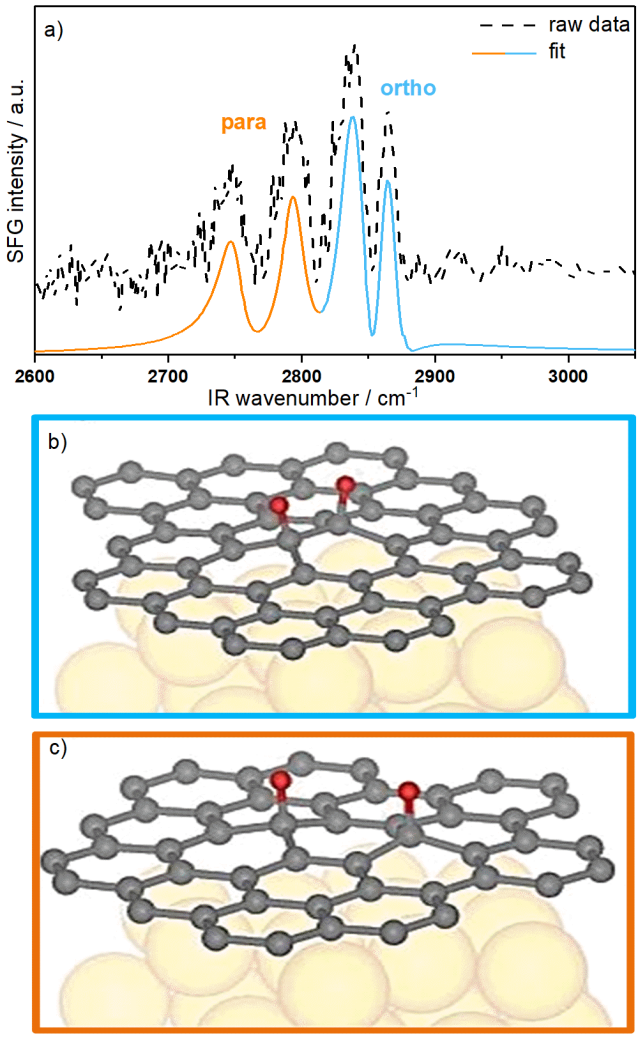

Figure 2. a) SFG spectra (after subtraction of the non-resonant background) of hydrogenated graphene at a coverage of 3.6% (black dashed line), and the best fit of the raw data to equation 1 in a colored solid line. The black raw spectrum is shifted upwards for clarity. Configuration of same-sided (*cis*) *ortho* (b, in blue) and *para* (c, in orange) hydrogen dimer on graphene on an Au(111) substrate according to DFT calculations with periodic boundary conditions applied.

The center IR wavenumbers extracted from these fits place the C-H vibrations at around 2740 cm^{-1}, 2785 cm^{-1}, 2840 cm^{-1}, and 2868 cm^{-1}, keeping in mind the resolution of our broadband-SFG spectrometer of around 15 cm^{-1}. It is clear that the C-H stretches on hydrogenated graphene

are red-shifted as compared to e.g. aliphatic C-H stretches which occur between 2850 and 3000 cm^{-1}. We indeed observe weak peaks at 2900 cm^{-1} and higher wavenumbers, see Figure 2, which are due to (polymeric) impurities due to the graphene transfer, and these can also be observed on our blank (i.e. non-hydrogenated) graphene samples, see Figure S3 in the supporting information.

The results are numerically also broadly in agreement with the previous SFG studies of Hasselbrink and co-workers (2560 cm^{-1} for *para* dimers, 2716 cm^{-1} for *ortho*, ~2847 cm^{-1} for mixed H/D functionalization)[19,40,41] and HREELS studies by Bisson and co-workers (2702 cm^{-1} for graph*ane* chair-like clusters and 2460 cm^{-1} for C-H dimers),[42] however, there is some discrepancy with regards to the assignment of the vibrational features. In order to correctly assign the vibrational peaks measured in this work, we have conducted DFT calculations of hydrogenated graphene on Au(111). We obtain harmonic frequencies at 2748 cm^{-1} and 2772 cm^{-1} (symmetric and anti-symmetric stretch, respectively) for *para* dimers and at 2847 cm^{-1} and 2876 cm^{-1} (anti-symmetric and symmetric stretch, respectively) for *ortho* dimers in which both H atoms adsorb from the same side (*cis*), away from the gold substrate, see Figure 2. To better compare these harmonic frequencies with the measured vibrational transition frequencies, we have performed molecular dynamics simulations (based on a realistic potential obtained from the *ab initio* calculations) at 300 K to reveal the difference between harmonic and anharmonic frequencies; we find that anharmonicity affects the bending modes quite severely, while anharmonic effects shift the vibrational frequencies of the stretching modes to the red by only ~12 cm^{-1}, around 40 cm^{-1} less than one obtains from an empirical Morse potential at dissociation energies of ~1.35 eV. We note that while we calculate Raman intensities which are more than 100 times larger for the symmetric stretches than for the anti-symmetric stretches for isolated

dimers, this ratio decreases to a factor between two and ten for clusters consisting of dimers on adjacent hexagonal rings. The calculated frequencies above are also close to those calculated by Sakong and Kratzer for dimers on free-standing graphene,[43] confirming that the weaker interaction between graphene and the gold substrate does not change harmonic frequencies significantly.

Modelling the adsorption from both sides, i.e. from above the graphene plane and from between the graphene and the gold substrate (*trans*), yields vibrational frequencies for the two possible dimers (we do not consider *meta* dimers based on unfavorable energetics) below 2700 cm^{-1} (*ortho*) and even below 2500 cm^{-1} (*para*) which we do not observe in our experiments. Furthermore, we calculated a gold-graphene separation distance of 3.42 Å; this is almost the same as the separation (~3.4 Å) of graphene from Ir(111) as employed by Lin *et al.*, Balgar *et al.*, and Balog *et al.*,[21,41,44] however, their H-graphene was prepared under vacuum, while we employed the wet-chemical Birch reduction;[53] here, the protons which attach to the graphene are solvated in a shell of ammonia molecules and – unlike isolated H atoms in the vacuum hydrogenation process – will be too large to diffuse between the graphene and gold, making double-sided hydrogenation less likely in our case. We also rule out adsorption of an odd number of hydrogen atoms (per benzene ring) based on unfavourable energetics and in agreement with previous theoretical work by Sakong *et al.* and Šljivančanin *et al.*[43,54]

Since two opposite H atoms (e.g. two *ortho* H atoms adsorbed from opposite sides of the graphene sheet) are not SFG-active due to their symmetry, one might assume that the weak SFG signal is due to this cancellation as pointed out by Hasselbrink and co-workers.[40] However, the weak SFG signal in our experiment is corroborated by the low coverages extracted from Raman spectroscopy, suggesting that on average one hydrogen atom is present for every five to 15

hexagonal rings. Clusters of higher hydrogen density have been proposed previously,[21,42,44] but our DFT calculations predict vibrational stretches below 2700 cm^{-1} for e.g. four hydrogen atoms adsorbed to one hexagonal ring, which we do not observe in our SFG experiments, such that we are confident to obtain homogenous coverages of 1% to 4% in our experiment.

Having established that single-sided hydrogen dimers in the *ortho* and *para* position are the most likely adsorption motifs under our experimental conditions, we focussed on the signal intensities of the peak at around 2740 cm^{-1} (the symmetric stretch of the *para* dimer) for four different samples which were hydrogenated for 45 s, 120 s, 300 s, and 360 s. These intensities can only be compared if the orientation of the C-H bond is the same for all samples, but this is likely the case here as the C-H bond would be (close to) perpendicular to the graphene plane for all coverages studied here. Most interestingly, the four fitted SFG spectra shown in Figure 3 (a) clearly show that the SFG peak intensity correlates with increasing hydrogenation time. SFG spectroscopy hence holds great potential to non-invasively measure the degree of surface functionalization on graphene; not only does the signal increase with coverage, but the frequency of the SFG signal also allows one to directly assign the type of functionalization.

Furthermore, we compared the SFG signal intensities for the four different samples with the coverages extracted from the Raman spectra, shown in Figure 3 (b) and summarized in Table 1. Due to the non-linear nature of the SFG process as shown in equation 1, we plotted the square-root of the SFG intensity as a function of the (Raman-extracted) coverage to yield a linear relationship, which could serve as a calibration to directly extract the coverage with (various) functional groups on graphene, which Raman cannot distinguish. We also observe a subtle red-shift of the SFG peak position with increasing intensity, however, this is within the resolution of

our SFG spectrometer, and one would not necessarily expect a shift of the peak position at coverages which only vary between 1% and 4%.

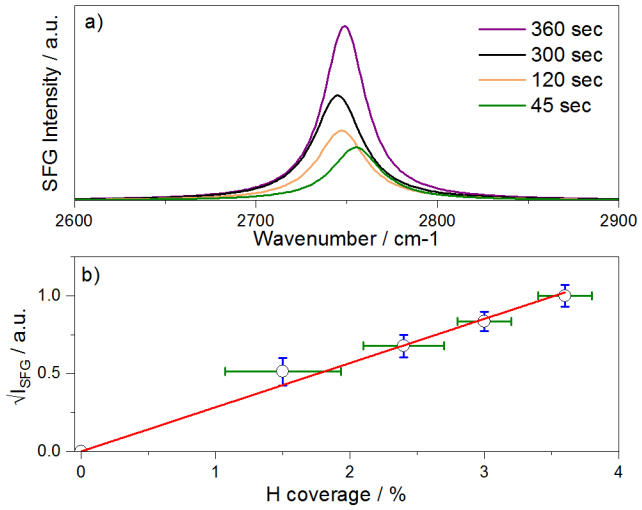

Figure 3. a) Fitted symmetric *para* peak from the SFG spectra of hydrogenated graphene after four different Birch reduction times. The intensities of the peaks increase as the coverage increases. b) Square-root of the SFG signal intensity of the C-H stretch as a function of the coverage derived from the corresponding Raman spectra, including a linear fit.

Table 1. Hydrogen coverages, peak intensities and frequencies for the symmetric C-H stretch at *para* position for four graphene samples hydrogenated for different reaction times.

.

Hydrogenation time / s	Hydrogen coverage / %	Relative SFG intensity / a.u.	$\tilde{\nu}_{SFG}$ / cm^{-1}
45	1.5 ± 0.4	0.51 ± 0.08	2744
120	2.4 ± 0.3	0.68 ± 0.07	2747
300	3.0 ± 0.2	0.84 ± 0.06	2745

360	3.6 ± 0.2	1.00 ± 0.07	2740

We briefly note that previous attempts in our group to hydrogenate graphene in a plasma chamber did not seem to create a high enough hydrogen coverage such that we failed to detect any C-H stretches, whereas the Birch reduction yields modest, but detectable levels of C-H covalent bonds on graphene, the SFG signals of which correlate with the Raman-derived surface coverages.

4. CONCLUSIONS

In summary, we report the preparation of partially hydrogenated graphene using the Birch reduction, and the subsequent characterization of the covalent C-H bonds on graphene by vibrational SFG spectroscopy. We assigned the detected C-H stretches to same-sided (*cis*) dimers in the *ortho* and *para* position guided by our DFT calculations of possible adsorption motifs. Significantly, the intensity of these vibrational features positively correlates with the Birch reduction times and hence surface coverages; this work thus paves the way for inferring properties such as e.g. the band gap in hydrogenated (or otherwise functionalized) graphene using a non-invasive technique such as SFG spectroscopy.

Notes

The authors declare no competing financial interests.

SUPPORTING INFORMATION

Hydrogen coverage calculations, Raman maps, and SFG spectra of non-hydrogenated CVD graphene on gold

ACKNOWLEDGEMENT

HAS thanks the Saudi government, the Royal Society of Chemistry (through the Sir Eric Rideal Trust) and the Association of British Spectroscopists Trust for funding. We also thanks Xin-Zheng Li (Peking University) and Angelos Michaelides (University College London) for very useful discussions, and one of the referees for excellent suggestions during the review process.

AUTHOR INFORMATION

*Huda AlSalem (huda.alsalem@postgrad.manchester.ac.uk) *Sven P. K. Koehler (s.koehler@mmu.ac.uk)

References:

(1) Novoselov, K. S.; Fal′ko, V. I.; Colombo, L.; Gellert, P. R.; Schwab, M. G.; Kim, K. A Roadmap for Graphene. *Nature* **2012**, *490*, 192–200.

(2) Randviir, E. P.; Brownson, D. A. C.; Banks, C. E. A Decade of Graphene Research: Production, Applications and Outlook. *Mater. Today* **2014**, *17*, 426–432.

(3) Gao, H.; Wang, L.; Zhao, J.; Ding, F.; Lu, J. Band Gap Tuning of Hydrogenated Graphene: H Coverage and Configuration Dependence. *J. Phys. Chem. C* **2011**, *115*, 3236–3242.

(4) Kuila, T.; Bose, S.; Mishra, A. K.; Khanra, P.; Kim, N. H.; Lee, J. H. Chemical Functionalization of Graphene and Its Applications. *Prog. Mater. Sci.* **2012**, *57*, 1061–1105.

(5) Zhang, S.; Yan, Z.; Li, Y.; Chen, Z.; Zeng, H. Atomically Thin Arsenene and Antimonene: Semimetal-Semiconductor and Indirect-Direct Band-Gap Transitions. *Angew. Chem Int. Ed.* **2015**, *54*, 3112–3115.

(6) Zhang, K.; Li, H.; Xu, X.; Yu, H. Facile and Efficient Synthesis of Nitrogen-Functionalized Graphene Oxide as a Copper Adsorbent and Its Application. *Ind. Eng. Chem. Res.* **2016**, *55*, 2328–2335.

(7) Baldovino, F. H.; Quitain, A. T.; Dugos, N. P.; Roces, S. A.; Koinuma, M.; Yuasa, M.; Kida, T. Synthesis and Characterization of Nitrogen-Functionalized Graphene Oxide in

High-Temperature and High-Pressure Ammonia. *RSC Adv.* **2016**, *6*, 113924–113932.

(8) Lee, H.; Cohen, M. L.; Louie, S. G. Selective Functionalization of Halogens on Zigzag Graphene Nanoribbons: A Route to the Separation of Zigzag Graphene Nanoribbons. *Appl. Phys. Lett.* **2010**, *97*, 233101.

(9) Xu, C.; Brown, P. A.; Lu, J.; Shuford, K. L. Electronic Properties of Halogen-Adsorbed Graphene. *J. Phys. Chem. C* **2015**, *119*, 17271–17277.

(10) Zheng, J.; Liu, H.-T.; Wu, B.; Di, C.-A.; Guo, Y.-L.; Wu, T.; Yu, G.; Liu, Y.-Q.; Zhu, D.-B. Production of Graphite Chloride and Bromide Using Microwave Sparks. *Sci. Rep.* **2012**, *2*, 00662.

(11) Hsiao, M. C.; Liao, S. H.; Yen, M. Y.; Liu, P. I.; Pu, N. W.; Wang, C. A.; Ma, C. C. M. Preparation of Covalently Functionalized Graphene Using Residual Oxygen-Containing Functional Groups. *ACS Appl. Mater. Interfaces* **2010**, *2*, 3092–3099.

(12) Schwartz, V.; Fu, W.; Tsai, Y.-T.; Meyer, H. M.; Rondinone, A. J.; Chen, J.; Wu, Z.; Overbury, S. H.; Liang, C. Oxygen-Functionalized Few-Layer Graphene Sheets as Active Catalysts for Oxidative Dehydrogenation Reactions. *ChemSusChem* **2013**, *6*, 840–846.

(13) Greenwood, J.; Phan, T. H.; Fujita, Y.; Li, Z.; Ivasenko, O.; Vanderlinden, W.; Van Gorp, H.; Frederickx, W.; Lu, G.; Tahara, K.; et al. Covalent Modification of Graphene and Graphite Using Diazonium Chemistry: Tunable Grafting and Nanomanipulation. *ACS Nano* **2015**, *9*, 5520–5535.

(14) Paulus, G. L. C.; Wang, Q. H.; Strano, M. S. Covalent Electron Transfer Chemistry of Graphene with Diazonium Salts. *Acc. Chem. Res.* **2013**, *46*, 160–170.

(15) Georgakilas, V.; Otyepka, M.; Bourlinos, A. B.; Chandra, V.; Kim, N.; Kemp, K. C.; Hobza, P.; Zboril, R.; Kim, K. S. Functionalization of Graphene: Covalent and Non-Covalent Approaches, Derivatives and Applications. *Chem. Rev.* **2012**, *112*, 6156–6214.

(16) Englert, J. M.; Dotzer, C.; Yang, G.; Schmid, M.; Papp, C.; Gottfried, J. M.; Steinrück, H. P.; Spiecker, E.; Hauke, F.; Hirsch, A. Covalent Bulk Functionalization of Graphene. *Nat. Chem.* **2011**, *3*, 279–286.

(17) Alsalem, H. S.; Holroyd, C.; Danial Iswan, M.; Horn, A. B.; Denecke, M. A.; Koehler, S. P. K. Characterisation, Coverage, and Orientation of Functionalised Graphene Using Sum-Frequency Generation Spectroscopy. *Phys. Chem. Chem. Phys.* **2018**, *20*, 8962–8967.

(18) Pumera, M.; Wong, C. H. A.; Williams, W. H.; Ecton, P. A.; Mo, Y.; Perez, J. M.; Loh, K. P.; Wang, S.; Lin, J.; Noréus, D.; et al. Graphane and Hydrogenated Graphene. *Chem. Soc. Rev.* **2013**, *42*, 5987.

(19) Kim, H.; Balgar, T.; Hasselbrink, E. The Stretching Vibration of Hydrogen Adsorbed on Epitaxial Graphene Studied by Sum-Frequency Generation Spectroscopy. *Chem. Phys. Lett.* **2011**, *508*, 1–5.

(20) Son, S.; Holroyd, C.; Clough, J.; Horn, A.; Koehler, S. P. K.; Casiraghi, C. Substrate

Dependence of Graphene Reactivity towards Hydrogenation. *Appl. Phys. Lett.* **2016**, *109*, 243103.

(21) Lin, C.; Feng, Y.; Xiao, Y.; Dürr, M.; Huang, X.; Xu, X.; Zhao, R.; Wang, E.; Li, X. Z.; Hu, Z. Direct Observation of Ordered Configurations of Hydrogen Adatoms on Graphene. *Nano Lett.* **2015**, *15*, 903–908.

(22) Kyhl, L.; Bisson, R.; Balog, R.; Groves, M. N.; Kolsbjerg, E. L.; Cassidy, A. M.; Jørgensen, J. H.; Halkjær, S.; Miwa, J. A.; Grubišić Čabo, A.; et al. Exciting H_2 Molecules for Graphene Functionalization. *ACS Nano* **2018**, *12*, 513–520.

(23) Castellanos-Gomez, A.; Wojtaszek, M.; Arramel; Tombros, N.; Van Wees, B. J. Reversible Hydrogenation and Bandgap Opening of Graphene and Graphite Surfaces Probed by Scanning Tunneling Spectroscopy. *Small* **2012**, *8*, 1607–1613.

(24) Eng, A. Y. S.; Sofer, Z.; Huber, Š.; Bouša, D.; Maryško, M.; Pumera, M. Hydrogenated Graphenes by Birch Reduction: Influence of Electron and Proton Sources on Hydrogenation Efficiency, Magnetism, and Electrochemistry. *Chem. Eur. J.* **2015**, *21*, 16828–16838.

(25) Feng, Y.; Chen, J.; Fang, W.; Wang, E. G.; Michaelides, A.; Li, X. Z. Hydrogenation Facilitates Proton Transfer through Two-Dimensional Honeycomb Crystals. *J. Phys. Chem. Lett.* **2017**, *8*, 6009–6014.

(26) Eng, A. Y. S.; Poh, H. L.; Šaněk, F.; Maryško, M.; Matějková, S.; Sofer, Z.; Pumera, M. Searching for Magnetism in Hydrogenated Graphene: Using Highly Hydrogenated Graphene Prepared via Birch Reduction of Graphite Oxides. *ACS Nano* **2013**, *7*, 5930–5939.

(27) Sarkar, A. K.; Saha, S.; Ganguly, S.; Banerjee, D.; Kargupta, K. Hydrogen Storage on Graphene Using Benkeser Reaction. *Int. J. Energy Res.* **2014**, *38*, 1889–1895.

(28) Spyrou, K.; Gournis, D.; Rudolf, P. Hydrogen Storage in Graphene-Based Materials: Efforts Towards Enhanced Hydrogen Absorption. *ECS J. Solid State Sci. Technol.* **2013**, *2*, M3160–M3169.

(29) Pumera, M. Graphene-Based Nanomaterials for Energy Storage. *Energy Environ. Sci.* **2011**, *4*, 668–674.

(30) Lucchese, M. M.; Stavale, F.; Ferreira, E. H. H. M.; Vilani, C.; Moutinho, M. V. O.; Capaz, R. B.; Achete, C. A.; Jorio, A. Quantifying Ion-Induced Defects and Raman Relaxation Length in Graphene. *Carbon* **2010**, *48*, 1592–1597.

(31) Beams, R.; Gustavo Cançado, L.; Novotny, L. Raman Characterization of Defects and Dopants in Graphene. *J. Phys. Condens. Matter* **2015**, *27*, 083002.

(32) Eckmann, A.; Felten, A.; Verzhbitskiy, I.; Davey, R.; Casiraghi, C. Raman Study on Defective Graphene: Effect of the Excitation Energy, Type, and Amount of Defects. *Phys. Rev. B* **2013**, *88*, 035426.

(33) Bekyarova, E.; Itkis, M. E.; Ramesh, P.; Berger, C.; Sprinkle, M.; de Heer, W. A.; Haddon, R. C. Chemical Modification of Epitaxial Graphene: Spontaneous Grafting of Aryl Groups. *J. Am. Chem. Soc.* **2009**, *131*, 1336–1337.

(34) Holroyd, C.; Horn, A. B.; Casiraghi, C.; Koehler, S. P. K. Vibrational Fingerprints of Residual Polymer on Transferred CVD-Graphene. *Carbon* **2017**, *117*, 473–475.

(35) Bain, C. D. Sum-Frequency Vibrational Spectroscopy of the Solid/Liquid Interface. *J. Chem. Soc., Faraday Trans.* **1995**, *91*, 1281–1296.

(36) Curtis, A. D.; Reynolds, S. B.; Calchera, A. R.; Patterson, J. E. Understanding the Role of Nonresonant Sum-Frequency Generation from Polystyrene Thin Films. *J. Phys. Chem. Lett.* **2010**, *1*, 2435–2439.

(37) Shen, Y. R. Surface Properties Probed by Second-Harmonic and Sum-Frequency Generation. *Nature* **1989**, *337*, 519–525.

(38) Lambert, A. G.; Davies, P. B.; Neivandt, D. J. Implementing the Theory of Sum Frequency Generation Vibrational Spectroscopy: A Tutorial Review. *Appl. Spectrosc. Rev.* **2005**, *40*, 103–145.

(39) Su, Y.; Han, H. L.; Cai, Q.; Wu, Q.; Xie, M.; Chen, D.; Geng, B.; Zhang, Y.; Wang, F.; Shen, Y. R.; et al. Polymer Adsorption on Graphite and CVD Graphene Surfaces Studied by Surface-Specific Vibrational Spectroscopy. *Nano Lett.* **2015**, *15*, 6501–6505.

(40) Balgar, T.; Kim, H.; Hasselbrink, E. Preparation of Graphene with Graphane Areas of Controlled Hydrogen Isotope Composition on Opposite Sides. *J. Phys. Chem. Lett.* **2013**, *4*, 2094–2098.

(41) Kim, H.; Balgar, T.; Hasselbrink, E. Is There Sp3-Bound H on Epitaxial Graphene? Evidence for Adsorption on Both Sides of the Sheet. *Chem. Phys. Lett.* **2012**, *546*, 12–17.

(42) Kyhl, L.; Balog, R.; Angot, T.; Hornekær, L.; Bisson, R. Hydrogenated Graphene on Ir(111): A High-Resolution Electron Energy Loss Spectroscopy Study of the Vibrational Spectrum. *Phys. Rev. B* **2016**, *93*, 115403.

(43) Sakong, S.; Kratzer, P. Hydrogen Vibrational Modes on Graphene and Relaxation of the C–H Stretch Excitation from First-Principles Calculations. *J. Chem. Phys.* **2010**, *133*, 054505.

(44) Balog, R.; Andersen, M.; Jørgensen, B.; Sljivancanin, Z.; Hammer, B.; Baraldi, A.; Larciprete, R.; Hofmann, P.; Hornekær, L.; Lizzit, S. Controlling Hydrogenation of Graphene on Ir(111). *ACS Nano* **2013**, *7*, 3823–3832.

(45) Li, M.; Wang, L.; Yu, N.; Sun, X.; Hou, T.; Li, Y. Structural Stability and Band Gap Tunability of Single-Side Hydrogenated Graphene from First-Principles Calculations. *J. Mater. Chem. C* **2015**, *3*, 3645–3649.

(46) Whitener, K. E.; Lee, W. K.; Campbell, P. M.; Robinson, J. T.; Sheehan, P. E. Chemical Hydrogenation of Single-Layer Graphene Enables Completely Reversible Removal of

Electrical Conductivity. *Carbon* **2014**, *72*, 348–353.

(47) Lagutchev, A.; Hambir, S. A.; Dlott, D. D. Nonresonant Background Suppression in Broadband Vibrational Sum-Frequency Generation Spectroscopy. *J. Phys. Chem. C* **2007**, *111*, 13645–13647.

(48) Kresse, G.; Furthmüller, J. Efficiency of Ab-Initio Total Energy Calculations for Metals and Semiconductors Using a Plane-Wave Basis Set. *Comput. Mater. Sci.* **1996**, *6*, 15–50.

(49) Blöchl, P. E. Projector Augmented-Wave Method. *Phys. Rev. B* **1994**, *50*, 17953–17979.

(50) Perdew, J. P.; Burke, K.; Ernzerhof, M. Generalized Gradient Approximation Made Simple. *Phys. Rev. Lett.* **1996**, *77*, 3865–3868.

(51) Payne, M. C.; Teter, M. P.; Allan, D. C.; Arias, T. A.; Joannopoulos, J. D. Iterative Minimization Techniques for *Ab Initio* Total-Energy Calculations: Molecular Dynamics and Conjugate Gradients. *Rev. Mod. Phys.* **1992**, *64*, 1045–1097.

(52) Wang, Q. H.; Jin, Z.; Kim, K. K.; Hilmer, A. J.; Paulus, G. L. C.; Shih, C. J.; Ham, M. H.; Sanchez-Yamagishi, J. D.; Watanabe, K.; Taniguchi, T.; et al. Understanding and Controlling the Substrate Effect on Graphene Electron-Transfer Chemistry via Reactivity Imprint Lithography. *Nat. Chem.* **2012**, *4*, 724–732.

(53) Birch, A. J. Reduction by Dissolving Metals. Part I. *J. Chem. Soc.* **1944**, 430–436.

(54) Šljivančanin, Ž.; Andersen, M.; Hornekær, L.; Hammer, B. Structure and Stability of Small H Clusters on Graphene. *Phys. Rev. B* **2011**, *83*, 205426.